

## Electronic Supplementary Information

### **Benzobisthiazole covalent organic framework photocatalysis for selective oxidation of benzyl amines**

Shengquan Zhu,<sup>a,†</sup> Hongxiang Zhao,<sup>a,†</sup> Yuexin Wang,<sup>a</sup> Zheng Li,<sup>a</sup> Siyu Zhang,<sup>a</sup> Bing Zeng,<sup>a</sup> Xue Zhou,<sup>a</sup> Xiang-Kui Gu<sup>b</sup> and Xianjun Lang<sup>a,\*</sup>

*<sup>a</sup>Hubei Key Lab on Organic and Polymeric Optoelectronic Materials, College of Chemistry and Molecular Sciences, Wuhan University, Wuhan 430072, China.*

*<sup>b</sup>School of Power and Mechanical Engineering, Wuhan University, Wuhan 430072, China.*

*<sup>†</sup>These authors contributed equally to this work.*

*\*To whom correspondence should be addressed. E-mail address:*

*[xianjunlang@whu.edu.cn](mailto:xianjunlang@whu.edu.cn) (Prof. X. J. Lang).*

## 1. Characterizations

Solid-state  $^{13}\text{C}$  cross-polarization/magic angle spinning nuclear magnetic resonance (CP-MAS NMR) experiments were performed on a Bruker AVANCE III 400 WB spectrometer operating at 100.62 MHz for  $^{13}\text{C}$  using a double resonance 4 mm MAS NMR probe and a sample spinning rate of 10 kHz. The cross-polarization time was 1 ms. The chemical shifts were referenced with trimethylsilane. The Fourier transform infrared spectroscopy (FTIR) was recorded from 400 to 4000  $\text{cm}^{-1}$  on Nicolet 5700 FTIR Spectrometer by using KBr pellets. All spectra were collected neatly in an ambient atmosphere. The signals are given in transmittance (%) against wavenumbers ( $\text{cm}^{-1}$ ). Powder X-ray diffraction (PXRD) measurement was carried out adopting a Rigaku/Miniflex 600 diffractometer with a filtered  $\text{Cu K}\alpha$  line, and the spectra were gathered from  $2^\circ$  to  $30^\circ$  at room temperature. The high-resolution transmission electron microscopy (HRTEM) images of COF photocatalysts were estimated on a JEOL JEM-2100 operating at an accelerating voltage of 200 kV. Field emission scanning electron microscopy (FE-SEM) was measured on a Zeiss Merlin Compact running at the acceleration voltage between 2 and 10 kV. The  $\text{N}_2$  isotherms and specific surface areas were determined at 77 K employing a Micromeritics ASAP 2460 automated system with the Brunauer–Emmet–Teller (BET) model, the samples were degassed in a vacuum ( $<1 \times 10^{-5}$  bar) at 120  $^\circ\text{C}$  for 8 h in the Micromeritics system before  $\text{N}_2$  physisorption. Meantime, porosity distributions were determined from the Nonlocal Density Functional Theory (NLDFIT) method. With  $\text{BaSO}_4$  as a reflectance standard,

the UV-vis DRS of covalent organic framework was estimated from 300–800 nm by a UV-3600 UV-vis spectrophotometer (Shimadzu, Japan) configured with a diffuse reflectance measurement accessory. The thermogravimetric analysis (TGA) curves were recorded on an SDT Q600 thermogravimeter from 30 °C to 800 °C at a rate of 10 °C/min under an N<sub>2</sub> atmosphere. After completion, the reaction mixture was detected by a gas chromatograph equipped with a flame ionization detector (GC-FID, Agilent 8890), using N<sub>2</sub> as the carrier gas and bromobenzene as the internal standard. The products were further verified by gas chromatography–mass spectrometry (GC-MS, Agilent 8890-5977B), using He as the carrier gas.

## **2. Chemical stability measurements**

The BBT-sp<sup>2</sup>c-COF samples (15 mg) were kept in 2 mL of DMF, THF, CH<sub>3</sub>OH, HCl (6 M) or NaOH (6 M), respectively for 7 d. The samples were washed with THF (for powders treated in organic solvents) or water (for powders treated in acid/base solutions), dried at 120 °C overnight under vacuum and subjected to PXRD measurement.

## **3. Electrochemical measurements**

Electrochemical measurements were executed on a Metrohm Autolab PGSTAT302N in a three-electrode electrochemical cell equipped with an electrochemical station. The working electrodes were prepared as follows: 2 mg of photocatalyst was dispersed in 1.0 mL absolute ethanol and 50 μL Nafion mixture

solution, which was ultrasonically dispersed for 30 min, and then 50  $\mu\text{L}$  of mixture solution was dropped onto the ITO with  $\pi \times (0.2)^2 \text{ cm}^2$  illuminated area and dried at room temperature, and the samples were dried under infrared irradiation. With 0.1 M  $\text{Na}_2\text{SO}_4$  aqueous solution supplied as the electrolyte, the Ag/AgCl electrode and platinum wire were the reference electrode and counter electrode, respectively. Meanwhile, the 3 W $\times$ 4 blue LEDs (Shenzhen Ouying Lighting Science and Technology Co., Ltd.) with a wavelength of  $460 \pm 10 \text{ nm}$  placed at 2 cm away from the photoelectrochemical cell were employed as the light source. The photocurrents were tested under blue LEDs irradiation with light on-off cycles at a time interval of 30 s and the scan rate was 100 mV/s. The electrochemical impedance spectroscopy (EIS) was carried out at a bias potential of + 0.5 V in the dark.

#### **4. Structure Modeling and PXRD Refinement of BBT-sp<sup>2</sup>c-COF**

Structural modeling of COFs was generated using the Accelrys Materials Studio 7.0 software package. The space groups were obtained from the Reticular Chemistry Structure Resource. The model was constructed in the initial lattice with the space group of P1. The proposed model was geometry optimized using the MS Forcite molecular dynamics module (Universal force fields, Ewald summations) to obtain the optimized lattice parameters. In addition, the atomic coordinate information was recorded according to the molecular module. Pawley refinement was applied to define the lattice parameters by Reflex module, producing the refined PXRD profile.

## 5. DFT calculations

The density functional theory (DFT) calculations were performed using the Gaussian 16, Revision C.01. Besides, the optimization and the point energy were implemented by B3LYP/6-31G(d,p) with correction terms in D3(BJ). The DOS were carried out through Multiwfn based on fchk of Gaussian 16.

## 6. Conversion and selectivity for the oxidation of amines to imine

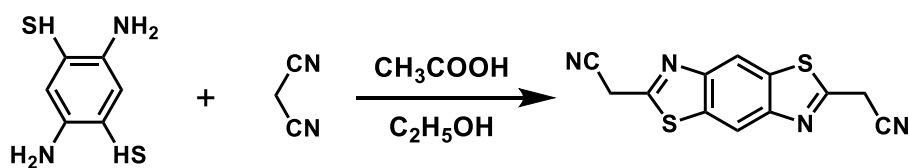
Conversion and selectivity for the oxidation of amines to imine were defined as follows:

$$\text{Conv. (\%)} = [(C_0 - C_s)/C_0] \times 100$$

$$\text{Sel. (\%)} = [C_p/(C_0 - C_s)] \times 100$$

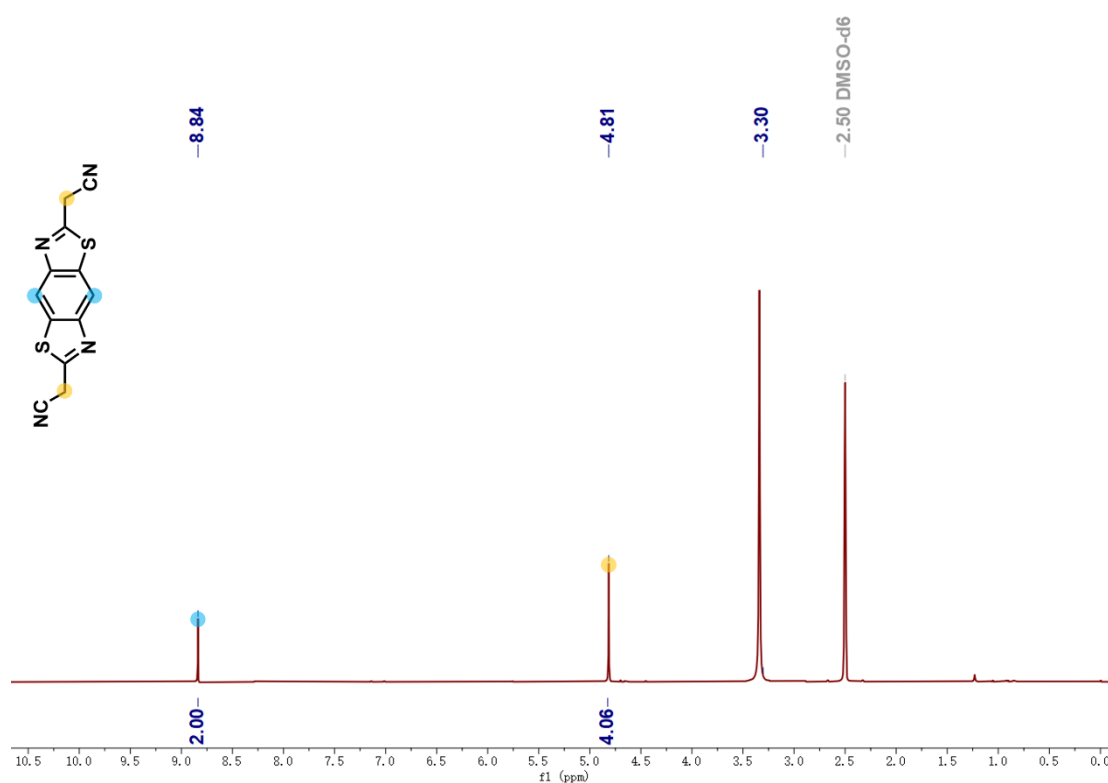
where  $C_0$  is the initial concentration of amine substrate, and  $C_s$  and  $C_p$  are the concentrations of substrate and imine product, respectively, at a certain time of the photocatalytic reaction.

## 7. Synthetic procedure of 2,2'-(benzo[1,2-d:4,5-d']bis(thiazole)-2,6-diyl)diacetonitrile<sup>1</sup>



2,5-Diamino-benzene-1,4-dithiol (1.083 g, 6.28 mmol), malononitrile (0.83 g, 12.6

mmol) and 754  $\mu\text{L}$  (13.1 mmol) glacial acetic acid were added into the solution of ethanol (25 mL). The mixture was degassed for 15 min and then refluxed for 3 d. The remaining solid was filtered off and washed with ethanol. Drying on vacuum yielded 1.468 g (5.43 mmol, 86%) as a grey solid.  $^1\text{H}$  NMR (400MHz,  $\text{DMSO-}d_6$ ):  $\delta$  8.84 (s, 2H),  $\delta$  4.06 (s, 4H).  $^1\text{H}$  NMR spectrum of BBT is shown as follows:



## 8. The exploration for the synthesis of the imine-linked COF

In order to explore a suitable contrast material, benzo[1,2-d:4,5-d']bisthiazole-2,6-diamine was designed and synthesized. The condensation reactions were carried out by utilizing benzo[1,2-d:4,5-d']bisthiazole-2,6-diamine and 1,3,6,8-tetrakis(4-formylphenyl)pyrene. At first, the reaction condition was controlled to be the same as before. However, the expected imine-linked COF didn't appear. Then a large number

of conditions were explored, including changing the type of solvent and controlling the volumes of solvent used. Eventually, the successful synthesis of the imine-linked COF is not realized no matter what conditions were adopted.

## 9. Supplementary Figures and Tables

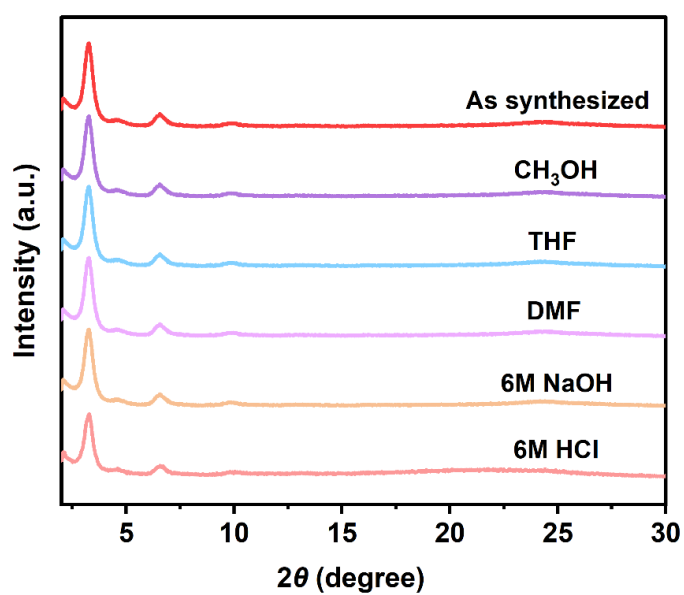


**Figure S1.** The PXRD peaks of BBT-sp<sup>2</sup>c-COF in different solvents.

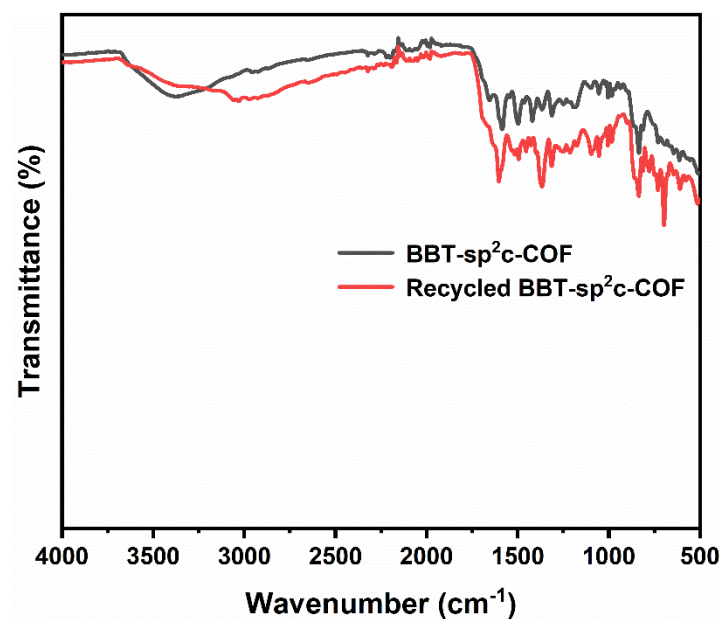


**Figure S2.** The FTIR spectra of BBT-sp<sup>2</sup>c-COF and recycled BBT-sp<sup>2</sup>c-COF.

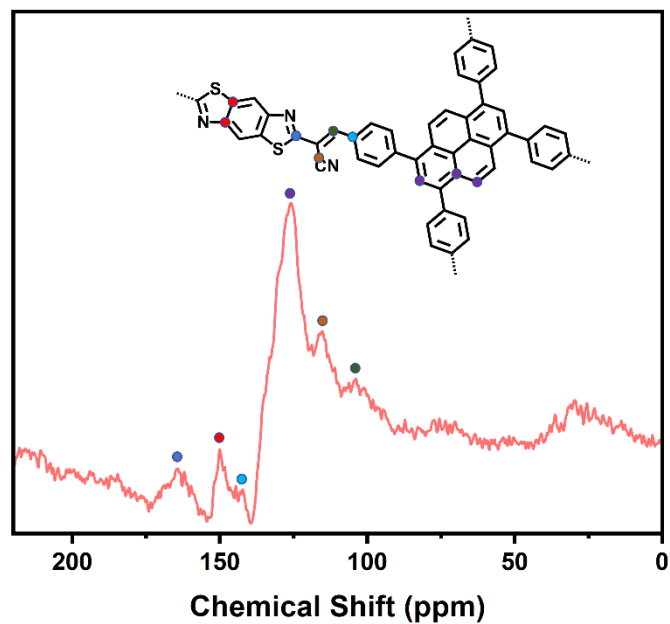


**Figure S3.** The solid-state <sup>13</sup>C NMR spectrum of BBT-sp<sup>2</sup>c-COF.

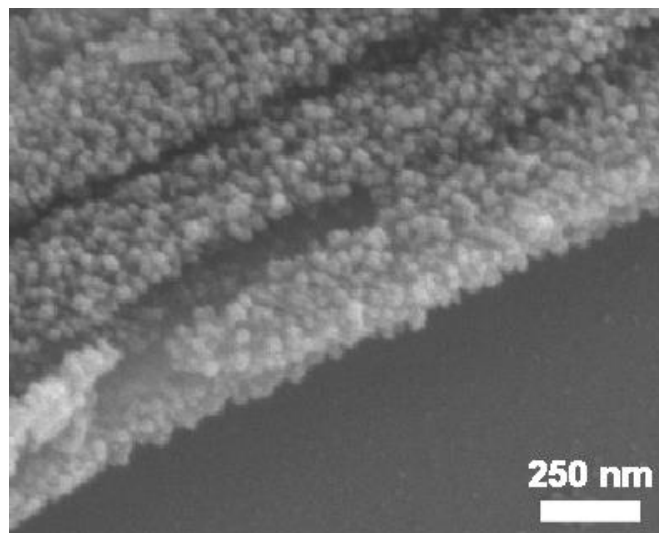


**Figure S4.** The SEM image of recycled BBT-sp<sup>2</sup>c-COF.

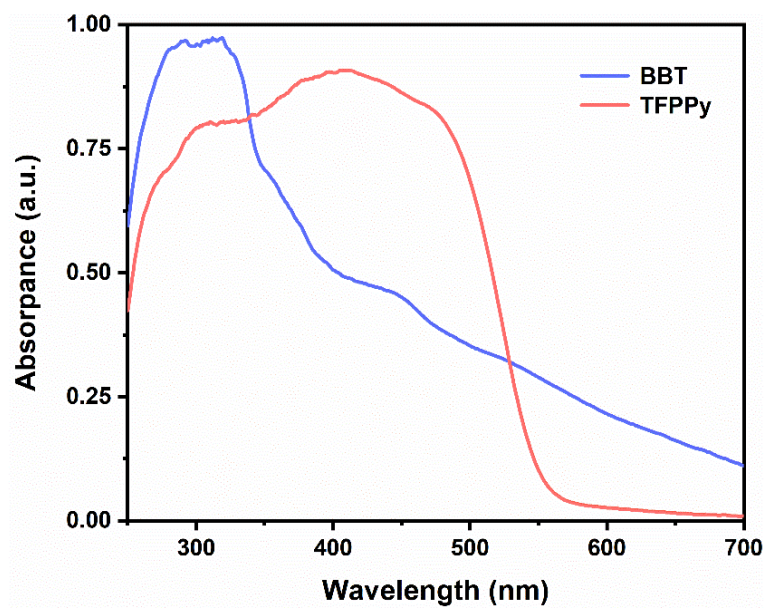


**Figure S5.** UV-vis DRS of BBT and TFPPy.

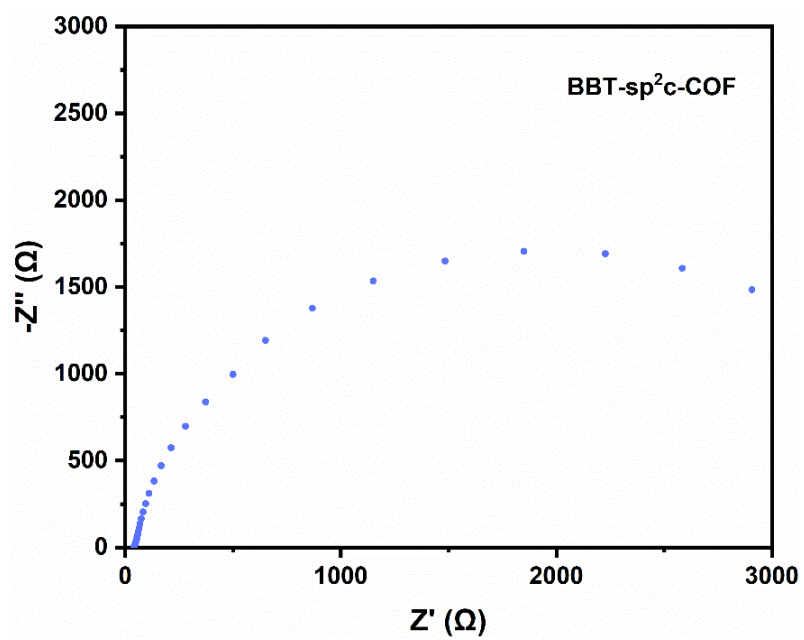


**Figure S6.** The EIS Nyquist plot of BBT-sp<sup>2</sup>c-COF.

**Table S1.** Blue light-driven selective oxidation of secondary amines by BBT-sp<sup>2</sup>c-COF photocatalysis.<sup>a</sup>

Entry	Substrate	Product	Conv. (%) <sup>b</sup>	Sel. (%) <sup>b</sup>
1			42	99
2			30	99
3			42	99
4			40	70
5			72	70

<sup>a</sup> Reaction conditions: BBT-sp<sup>2</sup>c-COF (5 mg), secondary amines (0.15 mmol), solvent (CH<sub>3</sub>CN, 1 mL), O<sub>2</sub> (0.1 MPa), 460 nm blue LEDs (3 W × 4), 1.8 h.

<sup>b</sup> Conversion and selectivity of secondary amines were determined by GC–FID.

**Table S2.** The impact of different solvents on the selective oxidation of benzylamine by BBT-sp<sup>2</sup>c-COF photocatalysis.<sup>a</sup>

Entry	Solvent	Conv. (%)	Sel. (%)
1	CH <sub>3</sub> CN	90	99
2	CH <sub>3</sub> OH	16	90
3	C <sub>2</sub> H <sub>5</sub> OH	43	73
4	DMF	88	99

<sup>a</sup> Reaction conditions: BBT-sp<sup>2</sup>c-COF (5 mg), benzylamine (0.3 mmol), blue LEDs (460 ± 10 nm, 3 W × 4), O<sub>2</sub> (0.1 MPa), 1.8 h.

**Table S3.** The photocatalytic activity of BBT for the selective oxidation of amines.<sup>a</sup>

Entry	Photocatalyst	Conv. (%)	Sel. (%)
1	BBT	29	99
2	BBT-sp <sup>2</sup> c-COF	90	99

<sup>a</sup> Reaction conditions: CH<sub>3</sub>CN (1 mL), photocatalyst, benzylamine (0.3 mmol), blue LEDs (460 ± 10 nm, 3 W × 4), O<sub>2</sub> (0.1 MPa), 1.8 h.

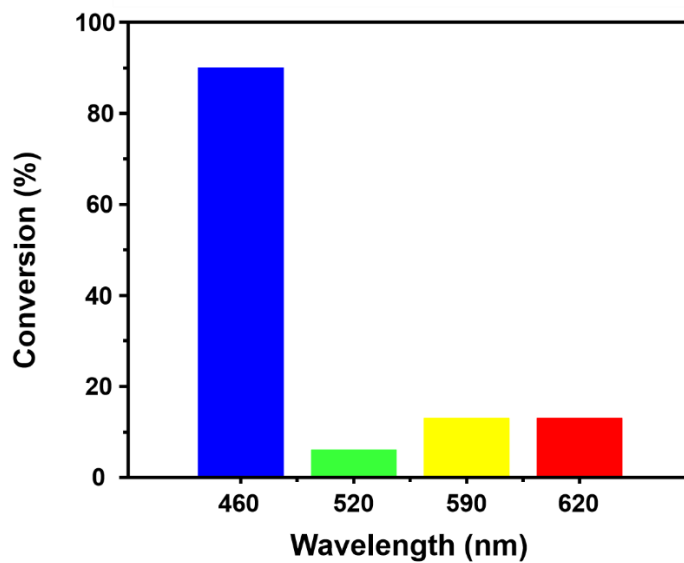


**Figure S7.** The influence of different peak wavelengths of LEDs on the selective oxidation of benzylamine by BBT-sp<sup>2</sup>c-COF photocatalysis.

**Table S4.** The influence of LED intensity on the selective oxidation of benzylamine by BBT-sp<sup>2</sup>c-COF photocatalysis.<sup>a</sup>

Entry	Intensity	Conv. (%)	Sel. (%)
1	12 W	90	99
2	9 W	75	99
3	6 W	47	99
4	3 W	18	99

<sup>a</sup> Reaction conditions: BBT-sp<sup>2</sup>c-COF (5 mg), benzylamine (0.3 mmol), blue LEDs (460 ± 10 nm), O<sub>2</sub> (0.1 MPa), 1.8 h.

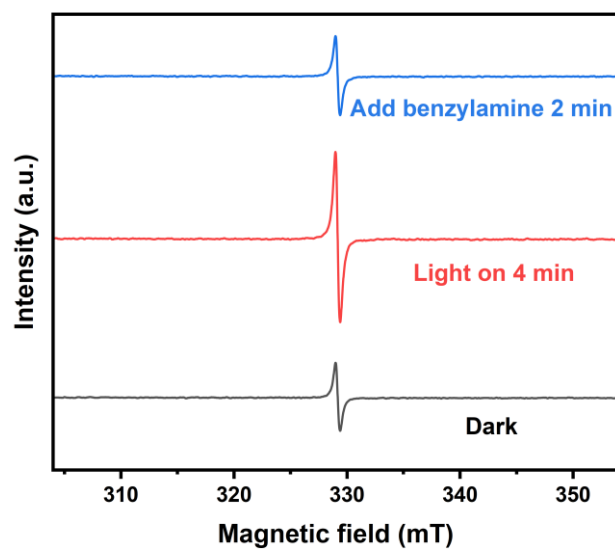


**Figure S8.** EPR signals of  $h^+$ .

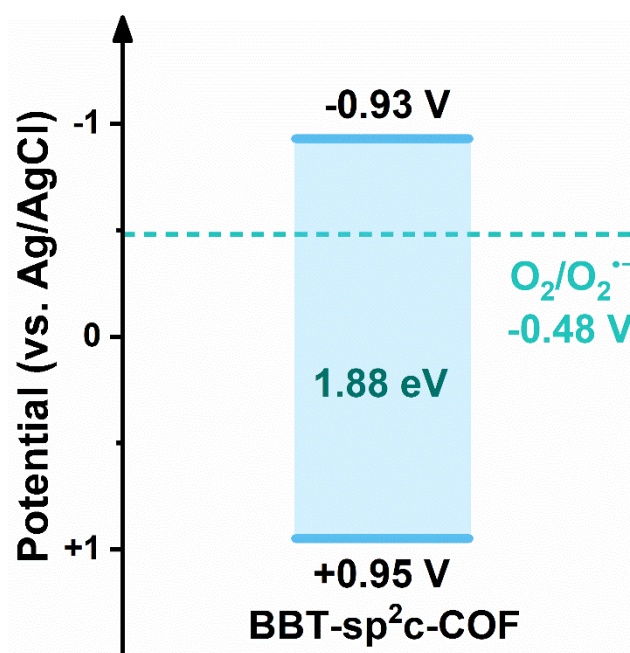


**Figure S9.** The band potentials of BBT-sp<sup>2</sup>c-COF and  $O_2/O_2^{\cdot-}$ .

**Table S5.** Fractional atomic coordinates for the unit cell of the BBT-sp<sup>2</sup>c-COF.

BBT-sp <sup>2</sup> c-COF							
AA Stacking				Space group: <i>P1</i>			
$a = 27.22 \text{ \AA}, b = 28.91 \text{ \AA}, c = 3.59 \text{ \AA}, \alpha = \beta = 90^\circ, \gamma = 84.12^\circ$							
Atom	x/a	y/b	z/c	Atom	x/a	y/b	z/c
C1	0.31349	-0.4206	0.12	C55	0.35642	-0.32439	0.544
C2	0.30531	-0.41103	0.734	C56	0.37296	-0.50499	0.094
C3	0.31129	-0.39974	1.308	C57	0.37651	-0.52922	-0.134
C4	0.32522	-0.39836	1.322	C58	0.37328	-0.5526	-0.198
C5	0.33356	-0.40791	0.699	C59	0.36181	-0.54546	0.098
C6	0.32733	-0.4189	0.076	C60	0.38134	-0.51522	0.135
C7	0.34843	-0.40562	0.574	C61	0.39494	-0.51291	-0.609
C8	0.35291	-0.39242	0.413	C62	0.46098	-0.42597	-1.109
C9	0.36631	-0.38919	0.151	C63	0.46759	-0.41438	-0.887
C10	0.37564	-0.3998	-0.029	C64	0.46059	-0.40193	-0.676
C11	0.37144	-0.41328	0.127	C65	0.48229	-0.41436	-0.719
C12	0.35804	-0.4161	0.504	C66	0.50211	-0.42301	-0.307
C13	0.38065	-0.42402	-0.097	C67	0.50515	-0.40953	-0.375
C14	0.37635	-0.43747	0.065	N1	0.26185	-0.41172	0.321
C15	0.36356	-0.43973	0.592	N2	0.38803	-0.3051	-0.101
C16	0.35478	-0.42931	0.837	N3	0.34537	-0.32634	0.828
C17	0.39820	-0.40779	-0.465	N4	0.29456	-0.4456	1.495
C18	0.39420	-0.42125	-0.436	N5	0.36359	-0.53222	0.135
C19	0.40320	-0.43205	-0.708	N6	0.40582	-0.51096	-0.952
C20	0.39808	-0.44511	-0.688	N7	0.48920	-0.42579	-0.503
C21	0.38514	-0.44818	-0.252	N8	0.45487	-0.39202	-0.503
C22	0.41807	-0.43068	-0.933	S1	0.25931	-0.43767	0.541
C23	0.42378	-0.42016	-1.672	S2	0.36476	-0.29459	0.472
C24	0.43763	-0.41836	-1.725	S3	0.38685	-0.54273	-0.442
C25	0.44624	-0.42757	-1.113	S4	0.4916	-0.3998	-0.688
C26	0.44074	-0.43893	-0.509	H1	0.30918	-0.42896	-0.414
C27	0.42689	-0.44032	-0.391	H2	0.30516	-0.39216	1.779

C28	0.38167	-0.46275	-0.115	H3	0.32941	-0.38985	1.842
C29	0.39112	-0.47171	0.426	H4	0.33300	-0.42591	-0.512
C30	0.38848	-0.48541	0.497	H5	0.34576	-0.38438	0.483
C31	0.37636	-0.49059	0.015	H6	0.36010	-0.44955	0.838
C32	0.36681	-0.48174	-0.497	H7	0.34538	-0.43183	1.299
C33	0.36951	-0.46806	-0.584	H8	0.40842	-0.40471	-0.560
C34	0.29053	-0.41186	0.666	H9	0.40451	-0.45324	-0.997
C35	0.28330	-0.4232	0.796	H10	0.41762	-0.41348	-2.246
C36	0.28949	-0.43567	1.183	H11	0.44157	-0.41008	-2.298
C37	0.23286	-0.43258	-0.028	H12	0.44719	-0.4463	-0.047
C38	0.24589	-0.42796	0.182	H13	0.42314	-0.44862	0.193
C39	0.24896	-0.4145	0.105	H14	0.40055	-0.46809	0.810
C40	0.23915	-0.40492	-0.174	H15	0.39580	-0.49186	0.962
C41	0.26866	-0.42314	0.57	H16	0.35734	-0.4855	-0.865
C42	0.37874	-0.33234	-0.033	H17	0.36203	-0.46174	-1.024
C43	0.40204	-0.28548	-0.283	H18	0.28531	-0.40253	0.486
C44	0.38982	-0.29187	-0.057	H19	0.23045	-0.4431	0.032
C45	0.37835	-0.28472	0.239	H20	0.24154	-0.39439	-0.225
C46	0.37852	-0.27076	0.325	H21	0.38922	-0.33013	-0.198
C47	0.37509	-0.30809	0.162	H22	0.41099	-0.29108	-0.517
C48	0.36977	-0.37456	0.065	H23	0.36957	-0.26516	0.556
C49	0.38129	-0.36927	0.678	H24	0.38791	-0.37559	1.245
C50	0.38421	-0.35563	0.608	H25	0.39326	-0.35192	1.076
C51	0.37520	-0.34672	0.018	H26	0.35661	-0.34526	-1.084
C52	0.36348	-0.35179	-0.565	H27	0.35202	-0.36909	-1.062
C53	0.36088	-0.36552	-0.553	H28	0.36260	-0.50726	0.324
C54	0.37023	-0.32209	0.192	H29	0.46674	-0.43513	-1.179

## Reference

1. G. M. Fischer, E. Daltrozzo and A. Zumbusch, *Angew. Chem. Int. Ed.*, 2011, **50**, 1406-1409.